

A novel core-shell structured upconversion nanorod as multimodal bioimaging and photothermal ablation agent for cancer theranostics

Chen Wang, ‡^{a,b} Chenlin Xu, ‡^a Liangge Xu,^a Chunqiang Sun,^a Dan Yang,^a Jiating Xu,^a Shili Gai,^{*a} Fei He,^a and Piaoping Yang^{*a}

^a Key Laboratory of Superlight Materials and Surface Technology, Ministry of Education, College of Material Sciences and Chemical Engineering, Harbin Engineering University, Harbin, 150001, P. R. China

^b School of Material Science and Technology, Jilin Institute of Chemical Technology, Jilin 132022, P. R. China

‡ C. W. and C. X. contributed equally.
*Email - yangpiaoping@hrbeu.edu.cn

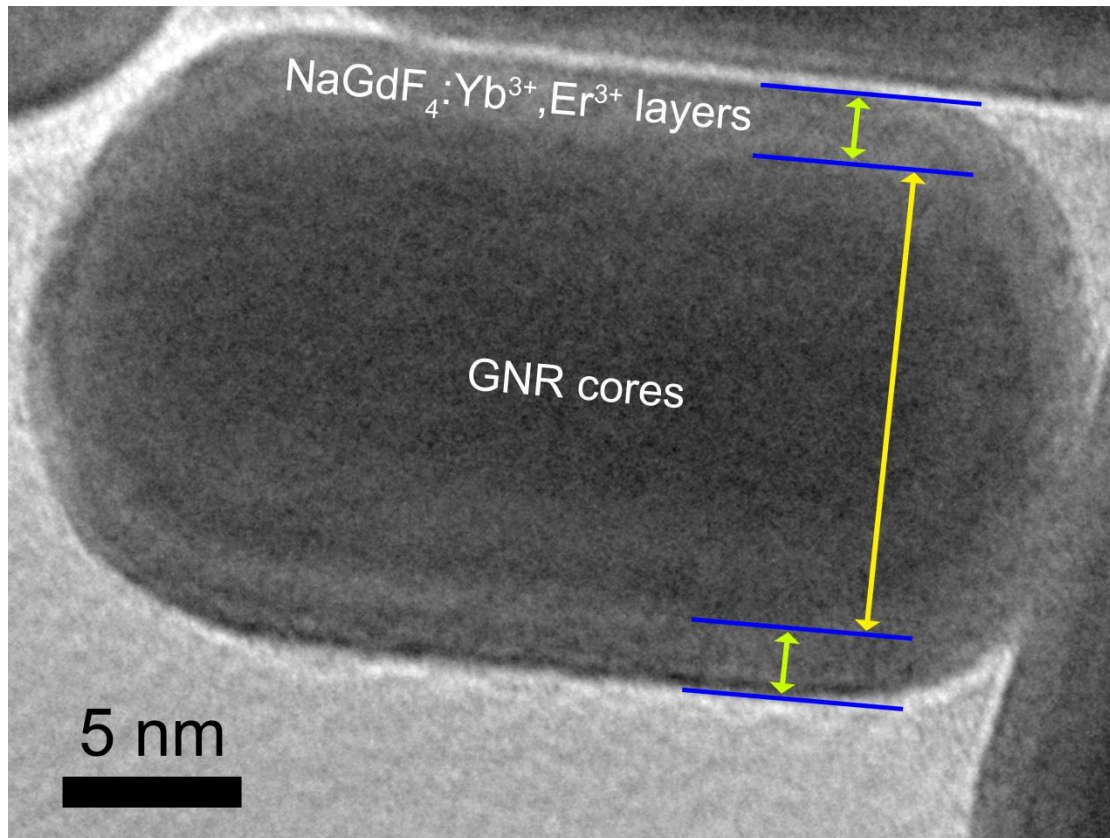


Fig. S1 Local enlarged TEM image of GNFNRs with related illustration of core-shell structure.

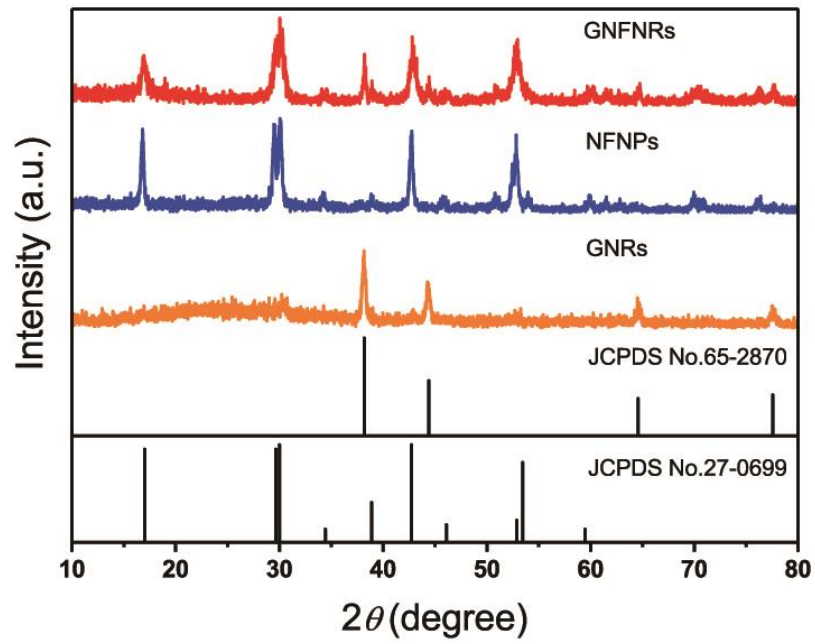


Fig. S2 XRD patterns of GNRs, NFNPs, and GNFNRs and relevant data lines of standard card are given for comparison.

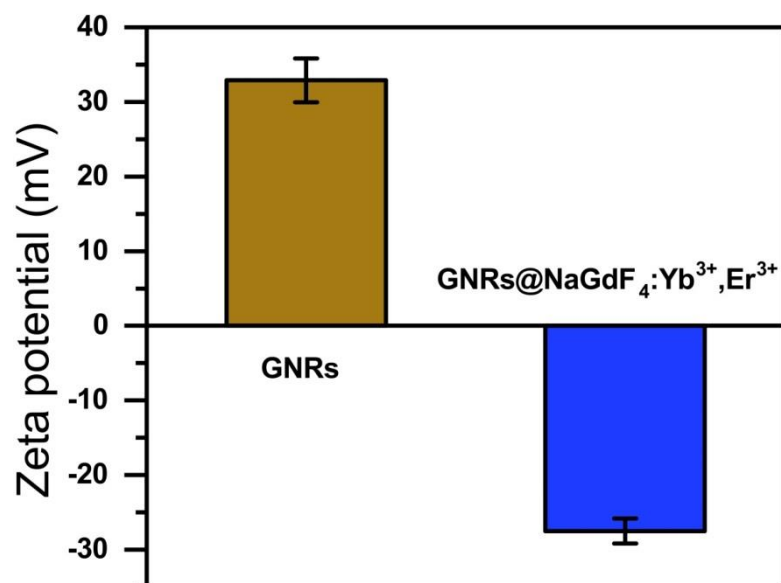


Fig. S3 Zeta potential of GNRs and GNRs@NaGdF₄:Yb³⁺,Er³⁺.

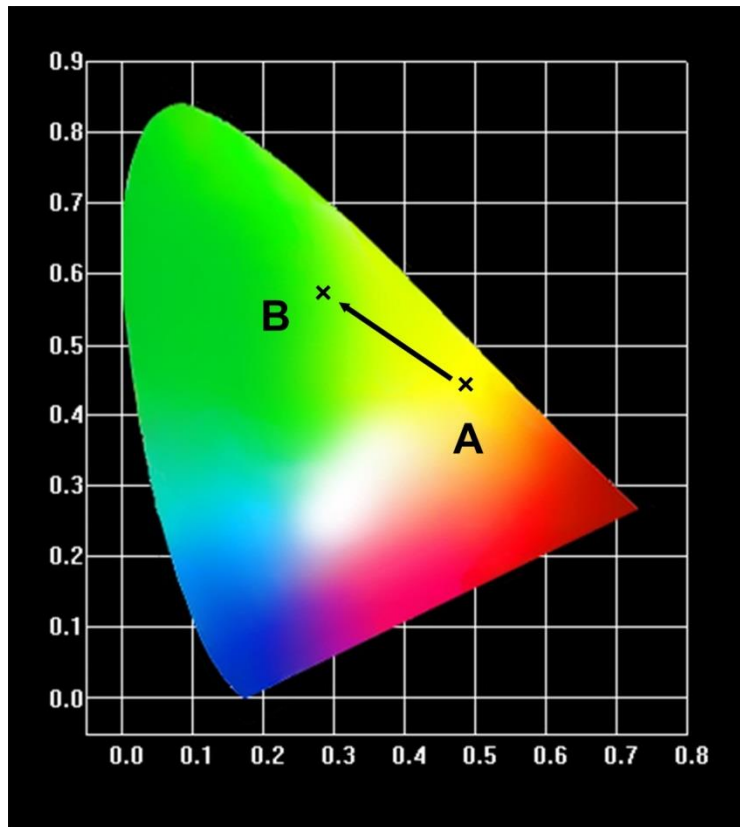


Fig. S4 CIE chromaticity diagram and the corresponding coordinate bits of both NFNPs (position A) and GNFNs (position B).

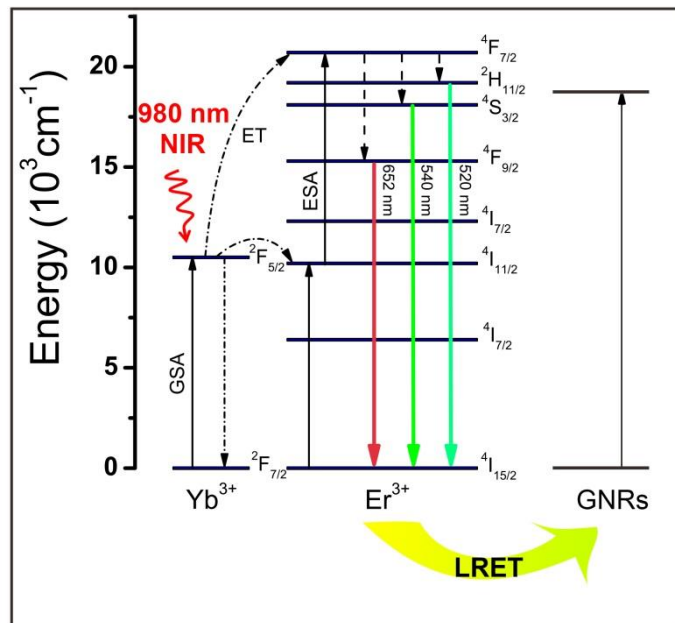


Fig. S5 Schematic of the energy level diagrams of $\text{Yb}^{3+}/\text{Er}^{3+}$ ions doped and energy transfer process with GNRs.

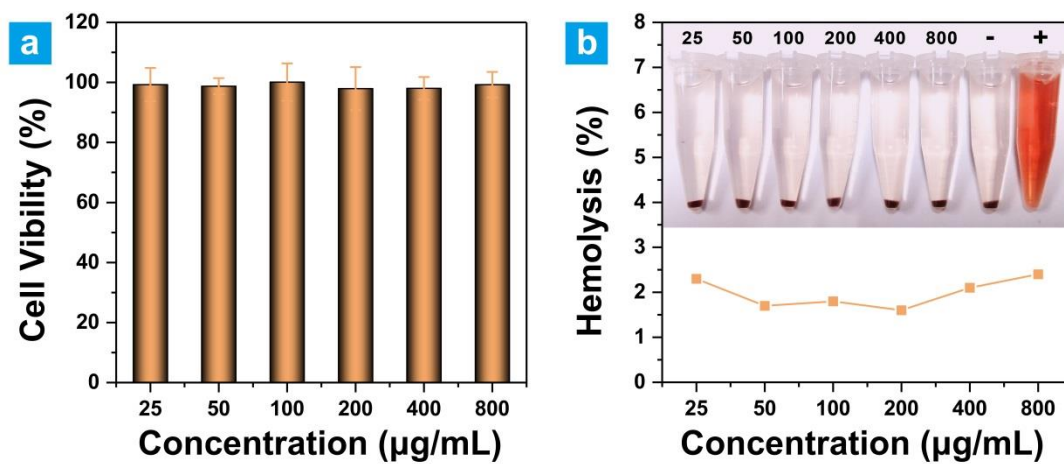


Fig. S6 Biocompatibility and hemolysis evaluation of GNFNRs. (a) L929 fibroblast cell viability in the presence of GNFNRs with different concentrations for 24 h. (b) Hemolytic assay of GNFNRs to human red blood cells.

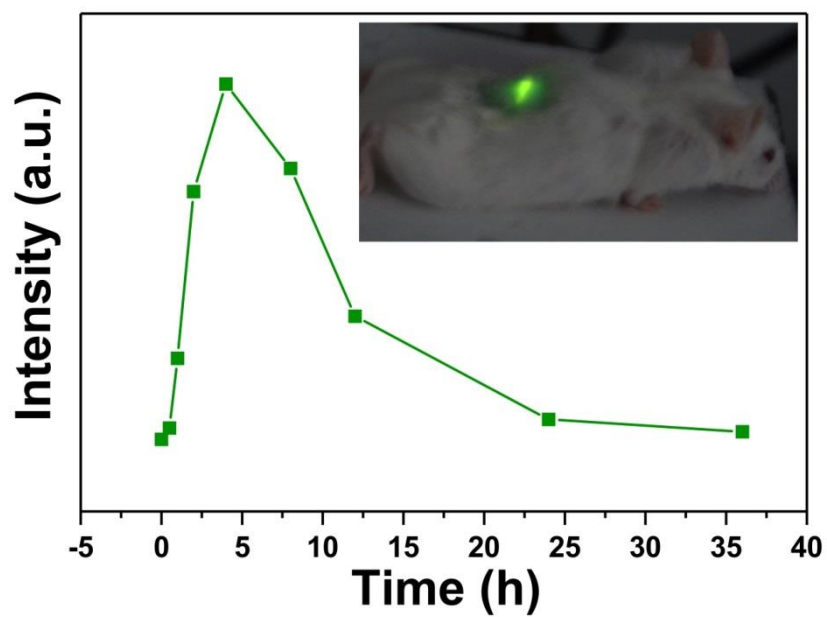


Fig. S7 The integrated intensity of UCL emission as a function of the tumor-bearing site injected time. (An *in vivo* merged images of a mouse injected with GNFNRs under NIR laser excitation is inset.)

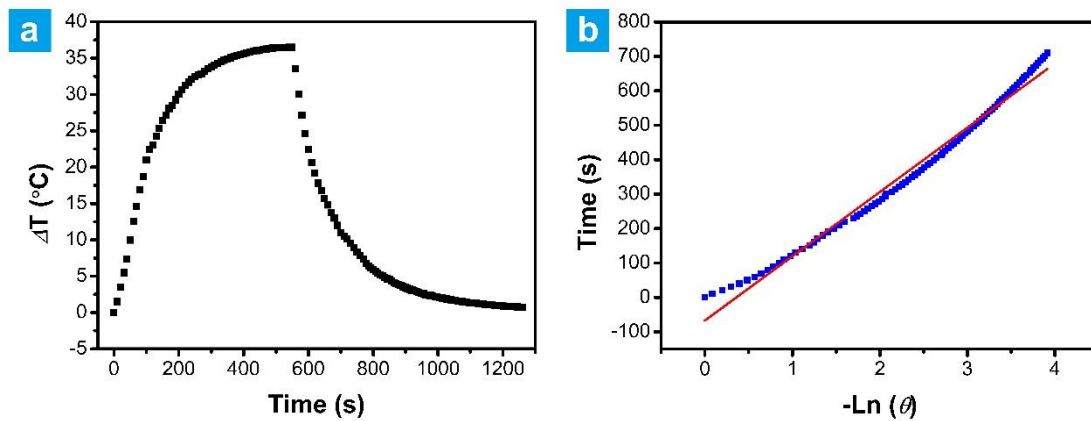


Fig. S8 The photothermal convert efficiency of the GNFNRs. (a) The photothermal response of the GNFNRs aqueous solution (200 $\mu\text{g}/\text{mL}$) for 500 s with 980 nm laser (0.6 W/cm^2) and then the laser was shut off. (b) Linear time data *versus* $-\ln(\theta)$ obtained from the cooling period of Fig. S7a.

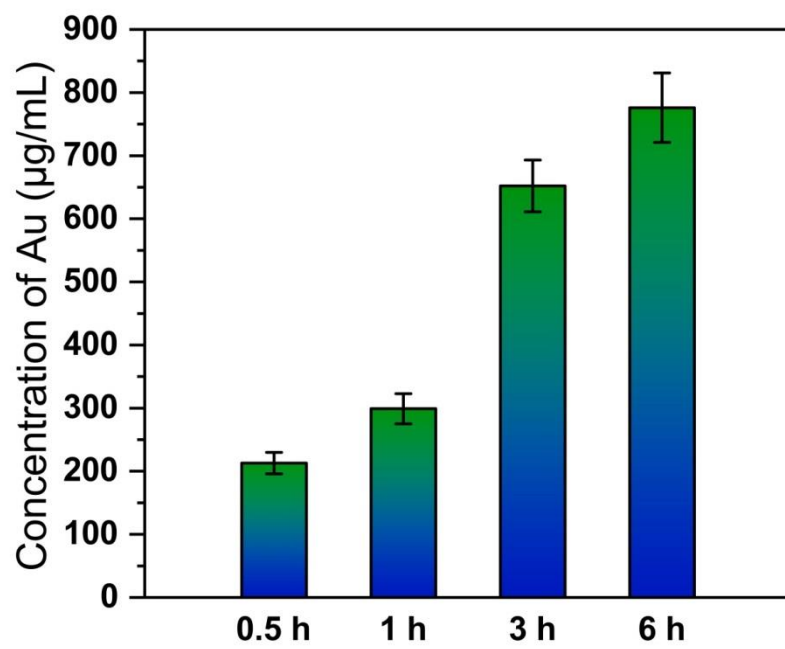


Fig. S9 Quantitative cellular uptake of HeLa cells at different times (n = 3).

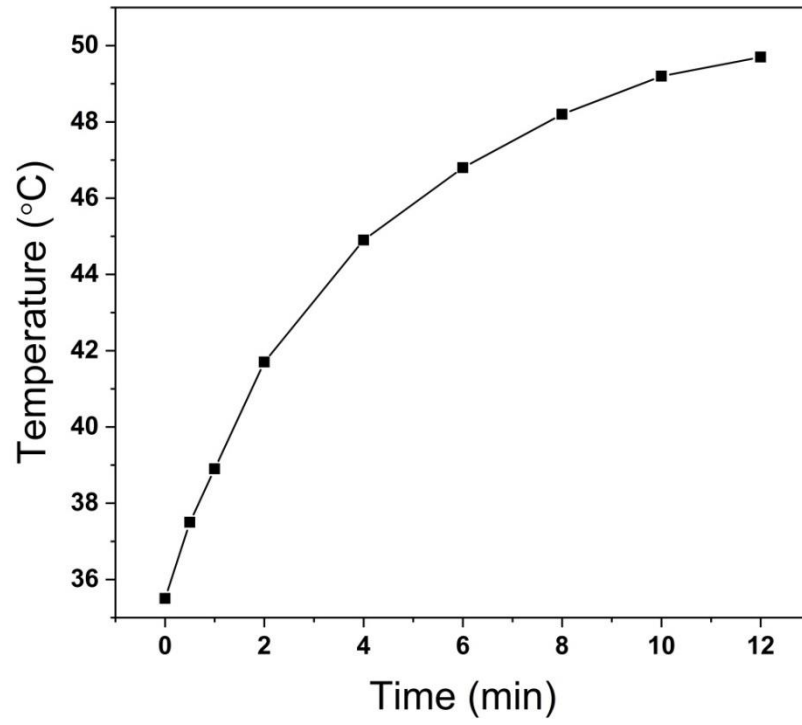


Fig. S10 *In vivo* temperature increase of the tumor-bearing mouse after injection with GNFNs under irradiation by a 980 nm laser.

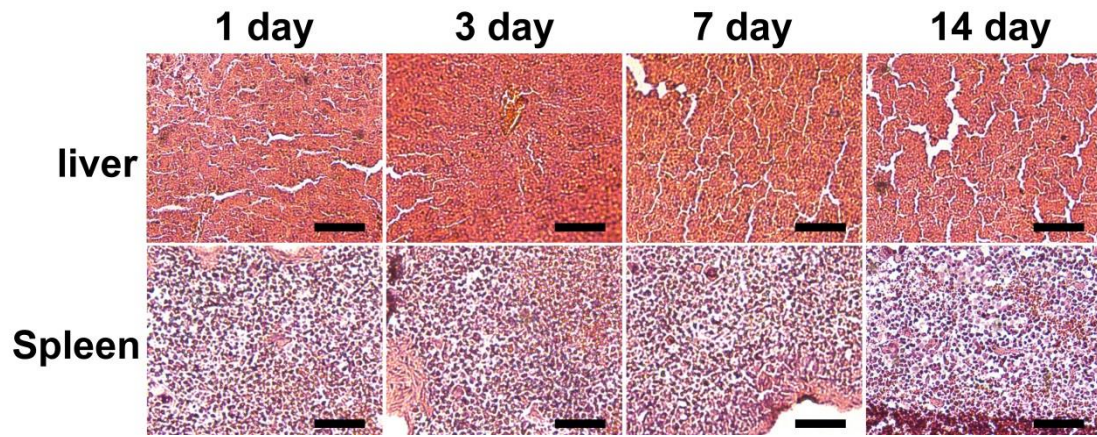


Fig. S11 H&E images of the kidneys and livers of the mice with different times.